Bitlis Eren Üniversitesi Fen Bilimleri Dergisi
BİTLİS EREN UNIVERSITY JOURNAL OF SCIENCE
ISSN: 2147-3129/e-ISSN: 2147-3188
VOLUME: 11 NO: 3 PAGE: 798-811 YEAR: 2022
DOI: 10.17798/bitlisfen.1102752

A Convolutional Neural Networks Model for Breast Tissue Classification

Mustafa Berkan BİÇER[1*], Hüseyin YANIK[2]

[1]*Electrical and Electronics Engineering, Engineering Faculty, Tarsus University, Tarsus, Mersin, Turkiye.*
[2]*Electrical and Electronics Engineering, Engineering Faculty, Mersin University, Mersin, Turkiye*
(ORCID: 0000-0003-3278-6071) (ORCID: 0000-0002-4386-5536)

Keywords: Breast tissue, classification, convolutional neural networks, machine learning, self-organizing fuzzy.

Abstract
The diagnosis of breast cancer and the determination of the cancer types are essential pieces of information for cancer research in monitoring and managing the disease. In recent years, artificial intelligence techniques have led to many developments in medicine, as any information about the patient has become more valuable. In particular, artificial intelligence methods used in the detection and classification of cancer tissues directly assist physicians and contribute to the management of the treatment process. This study aims to classify breast tissues with ten different tissue characteristics by utilizing the breast tissue data set, which has 106 electrical impedance spectroscopies taken from 64 patients in the UCI Machine Learning Repository database. Various machine learning algorithms including k-nearest neighbors, support vector machine, decision tree, self-organizing fuzzy logic, and convolutional neural networks are used to classify these tissues with an accuracy of 81%, 78%, 82%, 92%, and 96%, respectively. This study demonstrated the benefit of the usage of convolutional neural networks in cancer detection and tissue classification. Compared to traditional methods, convolutional neural networks provided better and more reliable results.

1. Introduction

Machine learning algorithms aim to analyze large data sets and intend to use the obtained information in a valuable way. Advances in machine learning and data processing techniques have directly affected many areas, especially the fields of the automotive [1], entertainment sector, digital markets [2], texture [3], fashion, defense [4] industries, and health [5]. Development of these algorithms leads to a variety of studies being done in these areas, especially in medicine.

The development of artificial intelligence techniques in parallel with technology has brought many developments in the field of health. These developments have made data on patients more valuable. Among these disease data sets, especially the analysis of data sets related to the diagnosis and classification of cancer diseases with artificial intelligence algorithms, produces direct results to help physicians and brings out results that will contribute to managing the treatment process.

Breast cancer is a type of cancer that grows slowly but can cause death rapidly when metastasizing and is the first leading cause of death after lung cancer among women with cancer in the world [6]. Research shows that the most important risk factor for the spread of breast cancer is the density of the breast tissue [7]. As with other types of cancer, the diagnosis of breast cancer at an early stage and the determination of cancerous tissue are of great importance in terms of monitoring the disease and implementing treatment.

It is known that the electrical impedance of breast tissue is compatible with the electrical properties of human tissue, which includes both resistance and capacitance, and that the electrical properties of biological tissues show significant

*Corresponding author: mberkanbicer@tarsus.edu.tr
Received: 13.04.2022, Accepted: 12.08.2022

differences depending on the structure and frequency [8]. Therefore, it is a complex and difficult process to define tissue characteristics using traditional methods. Advanced technical approaches provided by the developments in technology have become very useful in this context.

Electrical impedance techniques have emerged for use in obtaining and imaging tissue characteristics, have been used for a long time [9], and allow impedance mapping [10]. In a study presented by Jossinet in 1998 [10], significant differences were observed in the impedance and phase angle values in the examination between 6 different breast tissues in the range of 488 Hz to 1 MHz. These results suggest that electrical impedance spectroscopy (EIS) is a primary modality for classifying breast tissues and especially for the detection of breast cancer. Da Silva et al. proposed a breast tissue classification study using EIS [11]. Using the data obtained from 106 patients in an interventional way with EIS, the breast tissues were characterized and classified into 6 different types. Furthermore, a new data set was obtained in this study, which is called the UCI breast tissue data set [11]. Kerner et al. presented a classification study of breast tissue using EIS in 26 patients [12]. Images obtained from a multi-frequency EIS system are reconstructed using nonlinear differential equations, and an 83% performance rate is achieved on these images based on a special visual criterion.

Enachescu et al. presented a method based on the UCI breast tissue data set to detect and predict the presence of cancerous tissue in the breast [13]. In their study, the learning vector quantization (LVQ) method was used and an accuracy of 77% was obtained in the detection of breast tissue. Wu and Ng studied tissue classification on the UCI breast tissue data set using the radial-based function with different classifiers; naive bayes (NB), simple average (SA), and majority vote (MV). They achieved accuracies of 64%, 67%, 67%, and 80%, respectively [14].

In their study, Prasad et al. classified the UCI breast tissue data set by creating a fuzzy logic classification model, and an accuracy of 72% was achieved in the overall classification [15].

There are studies in the literature using hybrid algorithms. Alonso et al. tried to classify the UCI breast tissue data set using the logistic regression, NB, and the k-nearest neighbor (kNN) algorithms, and they achieved a success rate of 77% [16]. Also, the performance rate increased to 96% with a hybrid algorithm using a Bayesian approach. Daliri developed a hybrid algorithm by using the extreme learning machine (ELM) and support vector machines (SVM) methods and applied the hybrid algorithm to the UCI breast tissue data set [17]. In [17], an average value of 88% accuracy was obtained in classifying six different breast tissues in the data set. Eroğlu et al. classified the UCI breast tissue data set using ensemble learning algorithms such as random forest, SVM, and traditional artificial neural networks [18]. Using these methods, authors have achieved accuracies ranging from 76% to 83%. Liu et al. used the SVM algorithm for the classification of the UCI breast tissue data set and an average accuracy of 80% was obtained [19]. In the study of Ayyappan, breast tissue classification was carried out with different machine learning classifiers [20]. Since different results were obtained with different classifiers, the highest performance rate was obtained using bagging classification with 96%. Rahman et al. applied ensemble learning-based machine learning algorithms to the UCI breast tissue data set and classified different breast tissues [21]. The random forest (RF), decision trees (DT), AdaBoost, and gradient boosted regression trees have achieved 78%, 86%, 60%, and 75% success, respectively. Sadad et al. proposed a fuzzy c-means and region-growing based algorithm for segmentation and classification of tumours in mammograms [22]. Local binary pattern gray-level co-occurrence matrix and local phase quantization techniques were used to extract features [22]. A precision of 98.2% was achieved for the MIAS data set with DT and 95.8% was obtained for the DDSM data set using the kNN classifier [22]. Zhang et al. presented a convolutional neural network (CNN) based study to identify abnormal breast tissues taken from the MIAS data set [23]. An improved nine-layer CNN was proposed and a comparison of three activation functions; rectified linear unit (ReLU), leaky ReLU, and parametric ReLU, was made. In addition, six different pooling techniques were compared, and an accuracy of 94% was obtained with the combination of parametric ReLU and rank-based stochastic pooling.

In this study, different algorithms were utilized for the classification of breast tissues in the UCI breast tissue data set, and it was aimed to distinguish EIS measurements most efficiently. For this purpose, the classification accuracies of traditional algorithms such as SVM, kNN, and DT and advanced algorithms such as SOFLC and CNN were compared using the features of the breast tissue. Despite the fact that tissue classification and cancer detection studies have accelerated with the development of artificial neural network technology in recent years, one of the most important issues in CNN-based studies is that efficiency and cost are directly proportional. Therefore, attention is paid to keeping the efficiency high and maintaining the speed

of the algorithm while creating the CNN model. The question of whether the accuracy can be increased by using CNN for the UCI breast tissue data set has been the main motivation for this study. In addition to that, a new classifier called self-organizing fuzzy logic (SOFL) is applied to the same data set in order to evaluate the performance of it in such a highly used and cited data set.

2. Material and Method

In this study, it is aimed to classify six different breast tissues using UCI breast tissue data set [11] containing 106 different EIS measurements. Details concerning the data collection procedure are given in [10] and the properties of the data set can be seen in Table 1.

Table 1. Data set features

Parameter	Properties
Data set characteristic	Multivariate
Feature characteristic	Real number
Number of data	106
Number of features	10
Number of classes	6

The names and abbreviations of the six classes and the number of samples in each are given in Table 2. These samples were obtained from 64 different patients. In addition to that, the definitions of the features in the data set are given in Table 3. Using these features, the classification of six different breast tissues and detection of cancerous tissue can be done. Descriptive statistics for the data set are calculated for each feature and class in the data set, and given in the Table 4. As seen in Table 4, the range of values taken by each feature is at different levels. While the values of PA500 and HFS parameters are much less than 1, the values of Area, P, and I0 parameters are quite large.

Table 2. Breast tissue types and data population

Class	Abbreviation	Number of samples
Carcinoma	car	21
Fibroadenoma	fad	15
Mastopathy	mas	18
Glandular	gla	16
Connective	con	14
Adipose	adi	22

Table 3. Feature information of data set

Parameter	Details
I0	Impedivity (ohm) at zero frequency
PA500	Phase angle at 500 kHz
HFS	High-frequency slope of phase angle
DA	Impedance distance between spectral ends
Area	Area under spectrum
A/DA	Area normalized by impedance distance between spectral ends
Max IP	Maximum of the spectrum
DP	Distance between impedivity (ohm) at zero frequency and real part of the maximum frequency point
P	Length of the spectral curve
Class	6 different classes

The calculated correlation values between features are given in Table 5. When the correlation matrix given in Table 5 is examined, the features of P, DR, Area, and HFS features show high correlations with the I0 and Max IP, DA, A/DA, and PA500 features, respectively. The machine learning algorithms used in this study will be discussed in turn by considering the accuracy values obtained for test data. Statistics and confusion matrix plots regarding the results obtained with the presented classifiers are given in the Results and Discussion Section.

Table 4. Descriptive statistics for the data set

	Case	I0	PA500	HFS	DA	Area	A/DA	Max IP	DR	P	Class
Count	106.000	106.000	106.000	106.000	106.000	106.000	106.000	106.000	106.000	106.000	106.000
Mean	53.500	784.252	0.120	0.115	190.569	7335.155	23.474	75.381	166.711	810.638	3.500
Standard Deviation	30.744	753.950	0.069	0.101	190.801	18580.314	23.355	81.346	181.310	763.019	1.806
Minimum Value	1.000	103.000	0.012	-0.066	19.648	70.426	1.596	7.969	-9.258	124.979	1.000
1st Quartile	27.250	250.000	0.067	0.044	53.846	409.647	8.180	26.894	41.781	270.215	2.000
2nd Quartile	53.500	384.937	0.105	0.087	120.777	2219.581	16.134	44.216	97.833	454.108	3.000
3rd Quartile	79.750	1487.990	0.170	0.167	255.335	7615.205	30.953	83.672	232.990	1301.559	5.000
Maximum Value	106.000	2800.000	0.358	0.468	1063.441	174480.476	164.072	436.100	977.552	2896.583	6.000

Table 5. Correlation of the features in the data set

	I0	PA500	HFS	DA	Area	A/DA	Max IP	DR	P
I0	1.000	-0.394	0.029	0.820	0.560	0.612	0.824	0.733	0.989
PA500	-0.394	1.000	0.509	-0.090	0.084	0.230	-0.050	-0.077	-0.346
HFS	0.029	0.509	1.000	0.107	0.206	0.356	0.371	0.012	0.102
DA	0.820	-0.090	0.107	1.000	0.731	0.648	0.753	0.974	0.774
Area	0.560	0.084	0.206	0.731	1.000	0.830	0.735	0.676	0.574
A/DA	0.612	0.230	0.356	0.648	0.830	1.000	0.813	0.541	0.679
Max IP	0.824	-0.050	0.371	0.753	0.735	0.813	1.000	0.600	0.862
DR	0.733	-0.077	0.012	0.974	0.676	0.541	0.600	1.000	0.666
P	0.989	-0.349	0.102	0.774	0.574	0.679	0.862	0.666	1.000

2.1. Support Vector Machine

Support vector machine (SVM) is a vector space-based supervised artificial learning technique, adopted to solve the classification of single or multi-label data and regression problems, depending on the distance between two points in the data sets [24]. Although linear and nonlinear SVMs kernels can be applied according to the structure of the data, the linear SVM kernel is preferred in this study. While 76.42% of the data was used in the training of the presented SVM model, the remaining part of the data was used to test.

2.2. k-Nearest Neighbors (kNN)

Cover and Hart proposed the k-nearest neighbors (kNN) algorithm, which is one of the most widely used supervised machine-learning algorithms [25]. This algorithm is generally used in solving classification problems. It is generally used when all the features in a data set are continuous.

In kNN classification, firstly, the *k* value is determined in the algorithm. The *k* value corresponds to the number of elements to be examined. The distance between samples whose classes are known and new samples whose classes are tried to be found in the data set is calculated. Distances are computed using distance functions and sorted by their values. The nearest neighbors of the new sample are obtained, and the nearest class is selected based on distance functions. In this study, the Euclidean distance function (EDF) is used to perform the calculation as it is the most commonly used one in the literature. The mathematical expression of EDF is given in Eq. (1).

$$d(x,y) = \sqrt{\sum_{i=1}^{N} (x_i - y_i)^2} \quad (1)$$

d represents the distance between two points, and *x* and *y* denote the predicted and true values, respectively. There are many approaches to choosing the *k* value as it may vary depending on the data set. There are some important criteria when choosing the precise *k* value. Choosing a small *k* value causes noise to have bigger deflections on the result, while choosing a large *k* value increases the computational cost of the study. Generally, when trying different *k* values, the square root of the number of data points is taken as the upper limit value, and searching should start with a small value. The values between 1 and 10 as the *k* value were tried iteratively, and the value of 5 that gives the best accuracy for the classification problem was selected.

2.3. Decision Trees

Decision trees (DT) are relational probability maps in the form of a kind of tree. Quinlan inducts this algorithm and it helps to visualize and create feature thresholds based on decisions. In addition, DT demonstrates the best separation of a decision mathematically according to the characteristics of a data set [26].

Generally, a DT starts with a single node, and each node gives another opportunity to the next two possibilities, and the tree grows to the best separation. Nodes can vary between probability, decision, or end nodes based on their location.

DT classifiers classify as rule-based machine learning algorithms in multi and continuous feature data sets. Each decision tree branch is branched with feature-based threshold rules and causes new decisions that provide the opportunity to determine the correct class within the framework of these decisions.

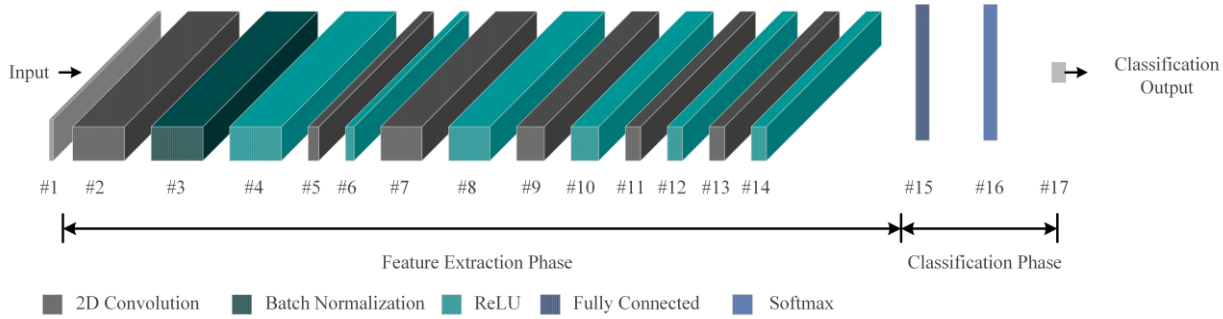

Figure 1. Proposed CNN classifier structure

2.4. Self-Organizing Fuzzy Logic Classifier (SOFLC)

The self-organizing fuzzy logic classifier (SOFLC) defines prototypes using input data via the offline training process [27]. In order to classify the data, it creates a 0-degree AnYa fuzzy rule-based system. After the first classification is done offline, the SOFLC model can update itself to fit the template of the new data by changing the system structure and meta-parameters as new data is generated. The values of the distance/dissimilarity parameter and granularity level were chosen as Euclidean and 34, respectively.

2.5. Convolutional Neural Networks

A convolutional neural network (CNN) is a multi-layered neural network structure that is often used in the feature extraction and classification of two-dimensional visual data and is an important part of the deep learning concept [28]. The differences between CNN and conventional neural networks (NN) are that CNN contains more layers than NNs and data features are extracted from the network structure. Hereby, the raw data to be classified can be given directly as an entry to the network. A CNN model can be easily applied to two-dimensional data such as images and videos. There are large CNN models developed and trained for various purposes in the literature. Despite some models are successful in classifying the training data, the accuracy of the model may be lower in different data sets or test data [28]–[30]. Therefore, it is important to design a CNN model suitable for the data, and learning parameters should be selected very carefully to prevent overfitting and underfitting as well. Since the breast tissue data set contains six different tissues, the output layer of the proposed CNN model has been selected to be a six-element classifier and the input layer is selected to be a nine-element. The constructed CNN model is shown in Figure 1. Details of the proposed CNN classifier and layers shown in Figure 1 are given in Table 6.

Table 6. Layer information about the proposed CNN model

#	Layer	Sizes	Learnable Parameter Sizes
1	Input	9×1×1	-
2	2D Convolution	9×1×93	Weights: 3×3×1×93 Biases: 1×1×93
3	Batch Normalization	9×1×93	Offset: 1×1×93 Scale: 1×1×93
4	ReLU	9×1×93	-
5	2D Convolution	9×1×48	Weights: 3×3×93×48 Biases: 1×1×48
6	ReLU	9×1×48	-
7	2D Convolution	9×1×89	Weights: 3×3×48×89 Biases: 1×1×89
8	ReLU	9×1×89	-
9	2D Convolution	9×1×68	Weights: 3×3×89×68 Biases: 1×1×68
10	ReLU	9×1×68	-
11	2D Convolution	9×1×55	Weights: 3×3×68×55 Biases: 1×1×55
12	ReLU	9×1×55	-
13	2D Convolution	9×1×55	Weights: 3×3×55×55 Biases: 1×1×55
14	ReLU	9×1×55	-
15	Fully Connected	1×1×6	Weights: 6×495 Biases: 6×1
16	Softmax	1×1×6	-
17	Classification Output	-	-

The initial weights for each layer of the CNN model are assigned using the *Xavier* weight initializer. The model was trained using 81 (76.42%) data points, and the remaining 25 (23.58%) data was used to test the model. In the training phase of the model, the number of data was kept the same, but after each training, the data was chosen randomly.

3. Results and Discussion

In this study, the UCI breast tissue data set was used, and by using this data set, the breast tissues were classified with the use of machine learning methods. In Table 7, methods used in classification, training

and test data distribution and performance rates are given.

Table 7. Classification performances

Classifiers	Accuracies (%)		
	Training	Test	All
SVM	83	88	84
kNN	81	92	84
DT	83	92	85
SOFLC	**83**	**92**	**85**
CNN	**100**	**96**	**99**

The DT structure and the chain of rules obtained in this study are illustrated in Figure 2. In this way, the relationship between properties and tissue characteristics can be observed. Also, evaluation metrics of the classifiers are computed using Eq. (2) – (9),

$$Accuracy = \frac{tp + tn}{tp + tn + fp + fn} \quad (2)$$

$$Sensitivity = \frac{tp}{tp + fn} \quad (3)$$

$$Specificity = \frac{tn}{tn + fp} \quad (4)$$

$$Precision = \frac{tp}{tp + fp} \quad (5)$$

$$False\ Positive\ Rate = \frac{fp}{fp + tn} \quad (6)$$

$$F_1\ score = \frac{2 \times tp}{2 \times tp + fp + fn} \quad (7)$$

$$MCC = \frac{tp \times tn - fp \times fn}{\sqrt{(tp + fp) \times (tp + fn) \times (tn + fp) \times (tn + fn)}} \quad (8)$$

$$Kappa = \frac{2 \times (tp \times tn - fn \times fp)}{(tp + fp) \times (fp + tn) \times (tp + fn) \times (fn + tn)} \quad (9)$$

where *tp*, *tn*, *fp* and *fn* represent *true positive (TP)*, *true negative (TN)*, *false positive (FP)* and *false negative (FN)*, respectively. While performing numerical calculations, the 5-fold cross-validation method was used. The training and test data, which are separated equally, were randomly chosen in each cycle, and the overall accuracy was calculated by averaging each accuracy value obtained in each fold. Accuracy, sensitivity, specificity, precision, false positive rate (FPR), F_1 score, Matthews correlation coefficient (MCC), and Cohen's Kappa values are calculated for each class separately and for all classes with the equations given with Eq (2) – (9) are tabulated in Table 8–12. As seen in Table 8, the accuracies of the SVM classifier were obtained as 82.7% and 88.0%, respectively, for training and testing. The MCC values range from 0.824 to 0.849 for training, test, and all data. These values show that there is an acceptable correlation between the predicted and the target classes.

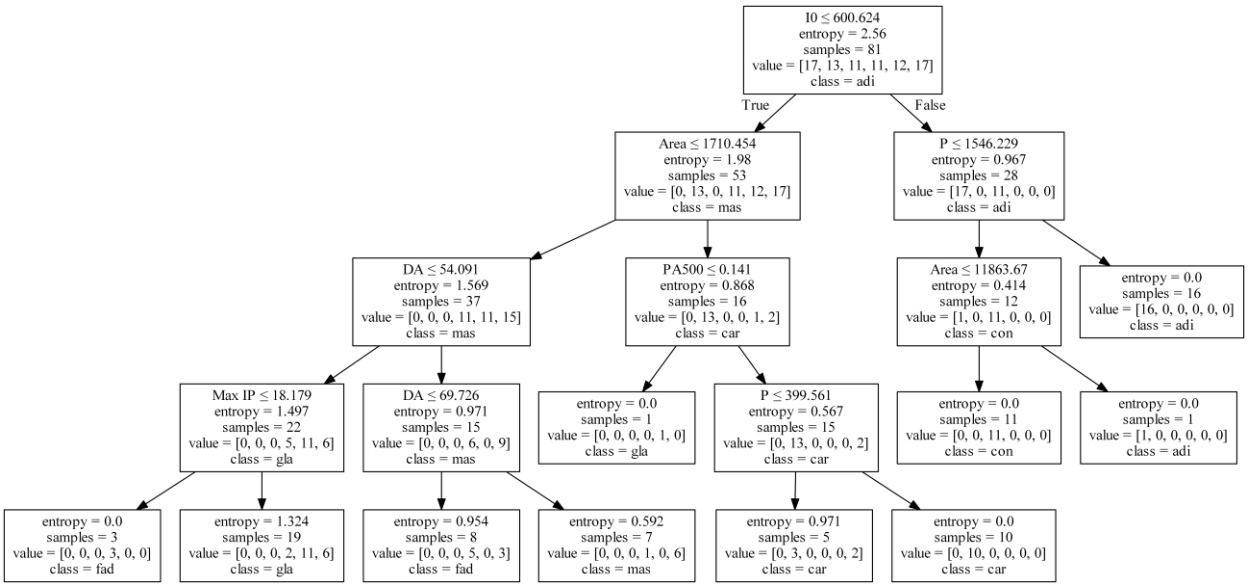

Figure 2. Decision tree and the rules identifying the relationship between features and tissues

Table 8. Detailed statistical results on SVM classification

	Class	Accuracy	Sensitivity	Specificity	Precision	FPR	F_1 score	MCC	Kappa	TP	FP	FN	TN
Train	Carcinoma	1.000	1.000	1.000	1.000	0.000	1.000	1.000	0.605	16	0	0	65
	Fibro-adenoma	0.938	0.938	0.938	0.789	0.062	0.857	0.823	0.583	15	4	1	61
	Mastopathy	1.000	1.000	1.000	1.000	0.000	1.000	1.000	0.753	10	0	0	71
	Glandular	0.667	0.667	0.971	0.800	0.029	0.727	0.689	0.739	8	2	4	67
	Connective	0.667	0.667	0.957	0.727	0.043	0.696	0.646	0.730	8	3	4	66
	Adipose	0.667	0.667	0.924	0.667	0.076	0.667	0.591	0.656	10	5	5	61
	All	0.827	0.823	0.965	0.831	0.035	0.824	0.791	0.378	-	-	-	-
Test	Carcinoma	1.000	1.000	1.000	1.000	0.000	1.000	1.000	0.520	6	0	0	19
	Fibro-adenoma	1.000	1.000	1.000	1.000	0.000	1.000	1.000	0.600	5	0	0	20
	Mastopathy	1.000	1.000	1.000	1.000	0.000	1.000	1.000	0.680	4	0	0	21
	Glandular	0.667	0.667	0.909	0.500	0.091	0.571	0.510	0.737	2	2	1	20
	Connective	0.750	0.750	1.000	1.000	0.000	0.857	0.846	0.725	3	0	1	21
	Adipose	0.667	0.667	0.955	0.667	0.045	0.667	0.621	0.770	2	1	1	21
	All	0.880	0.847	0.977	0.861	0.023	0.849	0.830	0.568	-	-	-	-
All	Carcinoma	1.000	1.000	1.000	1.000	0.000	1.000	1.000	0.585	22	0	0	84
	Fibro-adenoma	0.952	0.952	0.953	0.833	0.047	0.889	0.862	0.587	20	4	1	81
	Mastopathy	1.000	1.000	1.000	1.000	0.000	1.000	1.000	0.736	14	0	0	92
	Glandular	0.667	0.667	0.956	0.714	0.044	0.690	0.641	0.739	10	4	5	87
	Connective	0.688	0.688	0.967	0.786	0.033	0.733	0.692	0.729	11	3	5	87
	Adipose	0.667	0.667	0.932	0.667	0.068	0.667	0.598	0.682	12	6	6	82
	All	0.840	0.829	0.968	0.833	0.032	0.830	0.799	0.423	-	-	-	-

- Not Applicable.

When the Kappa values are examined, it shows that there is a moderate level of agreement, and there is also the possibility of chance during classification.

According to Table 9 regarding the kNN classifier, the accuracy for the training data was 81.5%, while the accuracy for the test data was 92%. In fact, since the kNN classifier does not contain a training phase, the most important factor determining the performance is the appropriate selection of training and test data. While the FPR parameter for this classifier had very low values, MCC results were obtained as 0.780 and 0.898 for training and test, respectively. These results show that the predicted classes had an acceptable correlation with the target classes. Also, it is seen that the kNN and SVM classifiers exhibit similar Kappa performance.

Table 9. Detailed statistical results on kNN classification

	Class	Accuracy	Sensitivity	Specificity	Precision	FPR	F_1 score	MCC	Kappa	TP	FP	FN	TN
Train	Carcinoma	0.857	0.857	0.985	0.923	0.015	0.889	0.868	0.674	12	1	2	66
	Fibro-adenoma	0.875	0.875	0.969	0.875	0.031	0.875	0.844	0.617	14	2	2	63
	Mastopathy	0.833	0.833	0.971	0.833	0.029	0.833	0.804	0.712	10	2	2	67
	Glandular	0.917	0.917	0.942	0.733	0.058	0.815	0.785	0.678	11	4	1	65
	Connective	1.000	1.000	0.942	0.750	0.058	0.857	0.841	0.663	12	4	0	65
	Adipose	0.467	0.467	0.970	0.778	0.030	0.583	0.539	0.721	7	2	8	64
	All	0.815	0.825	0.963	0.815	0.037	0.809	0.780	0.333	-	-	-	-
Test	Carcinoma	1.000	1.000	1.000	1.000	0.000	1.000	1.000	0.360	8	0	0	17
	Fibro-adenoma	1.000	1.000	0.950	0.833	0.050	0.909	0.890	0.570	5	1	0	19
	Mastopathy	1.000	1.000	1.000	1.000	0.000	1.000	1.000	0.840	2	0	0	23
	Glandular	1.000	1.000	1.000	1.000	0.000	1.000	1.000	0.760	3	0	0	22
	Connective	0.750	0.750	0.952	0.750	0.048	0.750	0.702	0.695	3	1	1	20
	Adipose	0.667	0.667	1.000	1.000	0.000	0.800	0.799	0.803	2	0	1	22
	All	0.920	0.903	0.984	0.931	0.016	0.910	0.898	0.712	-	-	-	-
All	Carcinoma	0.909	0.909	0.988	0.952	0.012	0.930	0.913	0.601	20	1	2	83
	Fibro-adenoma	0.905	0.905	0.965	0.864	0.035	0.884	0.855	0.606	19	3	2	82
	Mastopathy	0.857	0.857	0.978	0.857	0.022	0.857	0.835	0.741	12	2	2	90
	Glandular	0.933	0.933	0.956	0.778	0.044	0.848	0.826	0.697	14	4	1	87
	Connective	0.938	0.938	0.944	0.750	0.056	0.833	0.807	0.671	15	5	1	85
	Adipose	0.500	0.500	0.977	0.818	0.023	0.621	0.588	0.740	9	2	9	86
	All	0.840	0.840	0.968	0.837	0.032	0.829	0.804	0.423	-	-	-	-

- Not Applicable.

Table 10 contains detailed statistical classification results for the DT classifier. The accuracy values for the DT classifier were greater than 82.7%. The MCC values of the DT classifier, which exhibits similar Kappa performance to SVM and kNN, were also similar to the aforementioned models. When Table 11, which contains the results of the classification made using SOFLC, is examined, the accuracy values were in a similar range to those of SVM, kNN, and DT classifiers. On the other hand, the MCC and Kappa parameters had similarities with the mentioned models, although they have minor differences. In the SOFLC model, the MCC value for the test phase was higher than for the other models. The statistical values obtained by the proposed CNN model are shown in Table 12. When the values are examined, the model, which performs much better than previous models in terms of accuracy, sensitivity, and specificity, had the lowest FPR rates.

Table 10. Detailed statistical results on DT classification

	Class	Accuracy	Sensitivity	Specificity	Precision	FPR	F_1 score	MCC	Kappa	TP	FP	FN	TN
rain	Carcinoma	1.000	1.000	1.000	1.000	0.000	1.000	1.000	0.630	15	0	0	66
	Fibro-adenoma	1.000	1.000	1.000	1.000	0.000	1.000	1.000	0.654	14	0	0	67
	Mastopathy	1.000	1.000	1.000	1.000	0.000	1.000	1.000	0.753	10	0	0	71
	Glandular	0.857	0.857	0.910	0.667	0.090	0.750	0.698	0.626	12	6	2	61
	Connective	1.000	1.000	0.886	0.579	0.114	0.733	0.716	0.645	11	8	0	62
	Adipose	0.294	0.294	1.000	1.000	0.000	0.455	0.498	0.738	5	0	12	64
	All	0.827	0.859	0.966	0.874	0.034	0.823	0.819	0.378	-	-	-	-
Test	Carcinoma	1.000	1.000	1.000	1.000	0.000	1.000	1.000	0.440	7	0	0	18
	Fibro-adenoma	0.857	0.857	1.000	1.000	0.000	0.923	0.901	0.493	6	0	1	18
	Mastopathy	1.000	1.000	1.000	1.000	0.000	1.000	1.000	0.680	4	0	0	21
	Glandular	1.000	1.000	0.958	0.500	0.042	0.667	0.692	0.882	1	1	0	23
	Connective	0.800	0.800	1.000	1.000	0.000	0.889	0.873	0.648	4	0	1	20
	Adipose	1.000	1.000	0.958	0.500	0.042	0.667	0.692	0.882	1	1	0	23
	All	0.920	0.943	0.986	0.833	0.014	0.858	0.860	0.712	-	-	-	-
All	Carcinoma	1.000	1.000	1.000	1.000	0.000	1.000	1.000	0.585	22	0	0	84
	Fibro-adenoma	0.952	0.952	1.000	1.000	0.000	0.976	0.970	0.615	20	0	1	85
	Mastopathy	1.000	1.000	1.000	1.000	0.000	1.000	1.000	0.736	14	0	0	92
	Glandular	0.867	0.867	0.923	0.650	0.077	0.743	0.704	0.685	13	7	2	84
	Connective	0.938	0.938	0.911	0.652	0.089	0.769	0.737	0.648	15	8	1	82
	Adipose	0.333	0.333	0.989	0.857	0.011	0.480	0.487	0.774	6	1	12	87
	All	0.849	0.848	0.970	0.860	0.030	0.828	0.816	0.457	-	-	-	-

- Not Applicable.

Table 11. Detailed statistical results on SOFLC classification

	Class	Accuracy	Sensitivity	Specificity	Precision	FPR	F_1 score	MCC	Kappa	TP	FP	FN	TN
Train	Carcinoma	1.000	1.000	0.954	0.842	0.046	0.914	0.896	0.577	16	3	0	62
	Fibro-adenoma	0.727	0.727	0.957	0.727	0.043	0.727	0.684	0.740	8	3	3	67
	Mastopathy	0.286	0.286	0.970	0.667	0.030	0.400	0.369	0.767	4	2	10	65
	Glandular	1.000	1.000	0.928	0.706	0.072	0.828	0.809	0.653	12	5	0	64
	Connective	1.000	1.000	0.986	0.917	0.014	0.957	0.951	0.718	11	1	0	69
	Adipose	0.941	0.941	1.000	1.000	0.000	0.970	0.963	0.596	16	0	1	64
	All	0.827	0.826	0.966	0.810	0.034	0.799	0.779	0.378	-	-	-	-
Test	Carcinoma	1.000	1.000	1.000	1.000	0.000	1.000	1.000	0.600	5	0	0	20
	Fibro-adenoma	0.750	0.750	0.952	0.750	0.048	0.750	0.702	0.695	3	1	1	20
	Mastopathy	0.750	0.750	1.000	1.000	0.000	0.857	0.846	0.725	3	0	1	21
	Glandular	1.000	1.000	0.952	0.800	0.048	0.889	0.873	0.648	4	1	0	20
	Connective	1.000	1.000	1.000	1.000	0.000	1.000	1.000	0.760	3	0	0	22
	Adipose	1.000	1.000	1.000	1.000	0.000	1.000	1.000	0.600	5	0	0	20
	All	0.920	0.917	0.984	0.925	0.016	0.916	0.904	0.712	-	-	-	-
All	Carcinoma	1.000	1.000	0.965	0.875	0.035	0.933	0.919	0.582	21	3	0	82
	Fibro-adenoma	0.733	0.733	0.956	0.733	0.044	0.733	0.689	0.729	11	4	4	87
	Mastopathy	0.389	0.389	0.977	0.778	0.023	0.519	0.493	0.758	7	2	11	86
	Glandular	1.000	1.000	0.933	0.727	0.067	0.842	0.824	0.652	16	6	0	84
	Connective	1.000	1.000	0.989	0.933	0.011	0.966	0.961	0.728	14	1	0	91
	Adipose	0.955	0.955	1.000	1.000	0.000	0.977	0.971	0.597	21	0	1	84
	All	0.849	0.846	0.970	0.841	0.030	0.828	0.810	0.457	-	-	-	-

- Not Applicable.

The CNN model, which had the highest MCC values compared to the models examined within the scope of the study, also performed well according to the Kappa parameter, which is an indicator of compatibility. As it can be seen from the tables, the classifier with the lowest accuracy for test data was SVM, while the highest classifier performance was achieved by the proposed CNN model. While the lowest accuracy value was obtained with kNN in the classification of training and all data, the proposed CNN model reached the highest accuracy value. As it can be seen from the tables, the proposed CNN model shows great success in breast tissue classification.

Table 12. Detailed statistical results on CNN classification

	Class	Accuracy	Sensitivity	Specificity	Precision	FPR	F_1 score	MCC	Kappa	TP	FP	FN	TN
Train	Carcinoma	1.000	1.000	1.000	1.000	0.000	1.000	1.000	0.605	16	0	0	65
	Fibro-adenoma	1.000	1.000	1.000	1.000	0.000	1.000	1.000	0.728	11	0	0	70
	Mastopathy	1.000	1.000	1.000	1.000	0.000	1.000	1.000	0.654	14	0	0	67
	Glandular	1.000	1.000	1.000	1.000	0.000	1.000	1.000	0.704	12	0	0	69
	Connective	1.000	1.000	1.000	1.000	0.000	1.000	1.000	0.728	11	0	0	70
	Adipose	1.000	1.000	1.000	1.000	0.000	1.000	1.000	0.580	17	0	0	64
	All	1.000	1.000	1.000	1.000	0.000	1.000	1.000	1.000	-	-	-	-
Test	Carcinoma	0.800	0.800	1.000	1.000	0.000	0.889	0.873	0.648	4	0	1	20
	Fibro-adenoma	1.000	1.000	1.000	1.000	0.000	1.000	1.000	0.680	4	0	0	21
	Mastopathy	1.000	1.000	1.000	1.000	0.000	1.000	1.000	0.680	4	0	0	21
	Glandular	1.000	1.000	0.952	0.800	0.048	0.889	0.873	0.648	4	1	0	20
	Connective	1.000	1.000	1.000	1.000	0.000	1.000	1.000	0.760	3	0	0	22
	Adipose	1.000	1.000	1.000	1.000	0.000	1.000	1.000	0.600	5	0	0	20
	All	0.960	0.967	0.992	0.967	0.008	0.963	0.958	0.856	-	-	-	-
All	Carcinoma	0.952	0.952	1.000	1.000	0.000	0.976	0.970	0.615	20	0	1	85
	Fibro-adenoma	1.000	1.000	1.000	1.000	0.000	1.000	1.000	0.717	15	0	0	91
	Mastopathy	1.000	1.000	1.000	1.000	0.000	1.000	1.000	0.660	18	0	0	88
	Glandular	1.000	1.000	0.989	0.941	0.011	0.970	0.965	0.690	16	1	0	89
	Connective	1.000	1.000	1.000	1.000	0.000	1.000	1.000	0.736	14	0	0	92
	Adipose	1.000	1.000	1.000	1.000	0.000	1.000	1.000	0.585	22	0	0	84
	All	0.991	0.992	0.999	0.990	0.002	0.991	0.989	0.966	-	-	-	-

- Not Applicable.

Confusion matrix plots obtained utilizing the SVM, kNN, DT, SOFLC, and CNN classifiers are illustrated in Figure 3 (a) – (e).

(a)

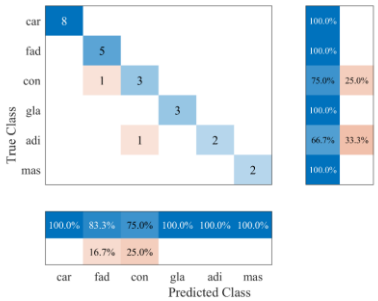

(b)

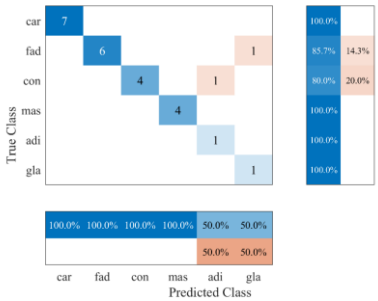

(c)

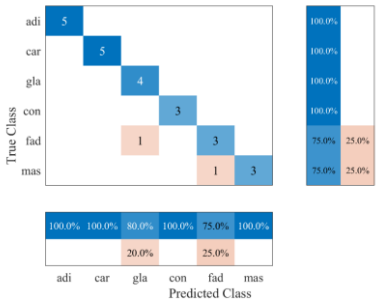

(d)

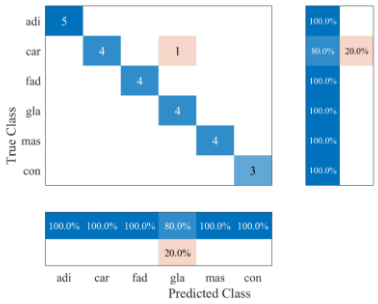

(e)

Figure 3. Confusion matrixes related to the classification result obtained from (a) SVM, (b) kNN, (c) DT, (d) SOFLC and (e) CNN classifiers

Table 13 shows the comparison of machine learning methods applied in this study with successful algorithms in the literature. Table 13 shows that the proposed CNN model gave the highest accuracy rate for training, test and entire data. In the classification of all tissues, it was observed that the SOFLC stands out in terms of overall speed and performance. In the classification between tumour tissue and normal tissue, CNN has achieved a success rate of 100% in training and 96% in test, showing the most successful result in determining tumour tissue. As a result, it is thought that increasing the number of samples in the data set will further stabilize the accuracy and increase the performance of CNN, especially in classification. The increase in the features in the data set along with the increase in the amount of data will also contribute to achieving better results in future studies.

Table 13. Test accuracy comparison of classification results with different approaches

	S1	**S2**	**S3**	**S4**	**S5**
(Wu and Ng 2007)	RBF	RBF+SA	RBF+MV	RBF+NB	-
	64.83%	66.81%	66.46%	80.27%	-
(Daliri 2015)	ELM	-	-	-	-
	88.95%	-	-	-	-
(Eroğlu et al. 2014)	SVM	RF	ANN	-	-
	81.13%	83.96%	76.41%	-	-
(Liu et al. 2015)	SVM	-	-	-	-
	80.62%	-	-	-	-
(Rahman et al. 2019)	RF	ERT	DT	GBT	ADB
	85.19%	81.48%	78.10%	74.08%	62.96%
This Study	SVM	kNN	DT	SOFLC	CNN
	88.00%	92.00%	92.00%	**92.00**%	**96.00**%

4. Conclusion and Suggestions

In this study, a convolutional neural network model having six convolution layers for breast tissue classification is proposed. The model was trained and tested using the breast tissue data set from UCI. To compare the performance of the proposed model, SVM, DT, kNN, and SOFLC models are also trained for classification using the same data set. The accuracy percentages for the classifier models SVM, kNN, DT, SOFLC, and the proposed CNN for the test data were obtained as 88%, 92%, 92%, and 96%, respectively. As compared to state-of-the-art methods used on this data set, the results demonstrated that the proposed model had a higher accuracy. The inclusion of six convolution layers with pooling layers in between, as well as the quantity of convolution filters, are the most significant factors that contribute to the proposed model's increased performance. A recently proposed technique called SOFLC was also utilized, and its performance was compared to that of conventional and convolutional neural networks. On the basis of accuracy and computational cost, SOFLC appears to be a promising method, although CNN outperforms in terms of total performance.

Contributions of the authors

The authors are equally contributed to the article.

Conflict of Interest Statement

There is no conflict of interest between the authors.

Statement of Research and Publication Ethics

The study is complied with research and publication ethics.

References

[1] T. Holleczek, C. Zysset, B. Arnrich, D. Roggen, and G. T. G, "Towards an interactive snowboarding assistance system," in International Symposium on Wearable Computers, September 4-7, 2009, pp. 147–148.

[2] T. T. Nguyen and G. Armitage, "A survey of techniques for internet traffic classification using machine learning," IEEE Commun. Surv. Tutor, vol. 10, no. 4, pp. 56-76.

[3] G. Cohen, S. Afshar, J. Tapson, and A. Schaik, "EMNIST: Extending MNIST to handwritten letters," in 2017 International Joint Conference on Neural Networks (IJCNN), May 14-19, 2017, pp. 2921–2926.

[4] A. L. Buczak and E. Guven, "A survey of data mining and machine learning methods for cyber security intrusion detection," IEEE Commun. Surv. Tutor, vol. 18, no. 2, pp. 1153-1176, 2016.

[5] A. Rajkomar, J. Dean, and I. Kohane, "Machine learning in medicine," N. Engl. J. Med, vol. 380, no. 14, pp. 1347-1358, 2019.

[6] C. E. DeSantis, S. A. Fedewa, A. G. Sauer, J. L. Kramer, R. A. Smith, and A. Jemal, "Breast cancer statistics, 2015: Convergence of incidence rates between black and white women," CA. Cancer J. Clin, vol. 66, no. 1, pp. 31-42, 2016.

[7] J. Jossinet and M. Schmitt, "A review of parameters for the bioelectrical characterization of breast tissue," Ann. NY. Acad. Sci, vol. 873, no. 1, pp. 30-41, 2006.

[8] S. Gabriel, R. W. Lau, and C. Gabriel, "The dielectric properties of biological tissues: III. Parametric models for the dielectric spectrum of tissues," Physics in Medicine and Biology, vol. 41, no. 11, pp. 2271-2293, 1996.

[9] W. K. Wg, "Impedance cardiography as a noninvasive means to monitor cardiac function," JAAMI J. Ass. Advan. Med. Instrum, vol. 4, no. 2, pp. 79-84, 1970.

[10] J. Jossinet, "The impedivity of freshly excised human breast tissue," Physiol. Meas, vol. 19, no. 1, pp. 61-75, 1998.

[11] J. E. Silva, J. P. M. Sá, and J. Jossinet, "Classification of breast tissue by electrical impedance spectroscopy," Med. Biol. Eng. Comput, vol. 38, no. 1, pp. 26-30, 2000.

[12] T. E. Kerner, K. D. Paulsen, A. Hartov, S. K. Soho, and S. P. Poplack, "Electrical impedance spectroscopy of the breast: clinical imaging results in 26 subjects," IEEE Trans. Med. Imaging, vol. 21, no. 6, pp. 638-645, 2002.

[13] D. Enachescu and C. Enachescu, "Learning vector quantization for breast cancer prediction," Portuguese conference on artificial intelligence, December 5-8, 2005, pp. 177–180.

[14] Y. Wu and S. C. Ng, "Combining neural learners with the naive bayes fusion rule for breast tissue classification," in 2nd IEEE Conference on Industrial Electronics and Applications, May 23-25, 2007, pp. 709–713.

[15] D. K. Prasad, C. Quek, and M. K. H. Leung, "A hybrid approach for breast tissue data classification," in TENCON 2009 – 2009 IEEE Region 10 Conference, Jan 23-27 2009, pp. 1–4.

[16] F. Calle-Alonso, C. J. Pérez, J. P. Arias-Nicolás, and J. Martín, "Computer-aided diagnosis system: A Bayesian hybrid classification method," Comput. Meth. Prog. Bio, vol. 112, no. 1, pp. 104-113, 2013.

[17] M. R. Daliri, "Combining extreme learning machines using support vector machines for breast tissue classification," Comput. Methods Biomech. Biomed. Eng, vol. 18, no. 2, pp. 185-191, 2015.

[18] K. Eroğlu, E. Mehmetoglu, and N. Kılıç, "Success of ensemble algorithms in classification of electrical impedance spectroscopy breast tissue records," in 22nd Signal Processing and Communications Applications Conference (SIU), April 23-25, 2014, pp. 1419–1422.

[19] C. Liu, T. Chang, and C. Li, "Breast tissue classification based on electrical impedance spectroscopy," in Proceedings of the 2015 International Conference on Industrial Technology and Management Science, 2015, pp. 237–240.

[20] G. A. Ayyappan and K. S. Kumar, "Novel classification approach-1 on breast tissue dataset," Indian Journal of Computer Science and Engineering, vol. 9, no. 4, pp. 115-118, 2018.

[21] S. M. Rahman, M. A. Ali, O. Altwijri, M. Alqahtani, N. Ahmed, and N. U. Ahamed, "Ensemble-based machine learning algorithms for classifying breast tissue based on electrical impedance spectroscopy," in Advances in Artificial Intelligence, Software and Systems Engineering, Cham, 2020, pp. 260–266.

[22] T. Sadad, A. Munir, T. Saba, and A. Hussain, "Fuzzy C-means and region growing based classification of tumor from mammograms using hybrid texture feature," J. Comput. Sci, vol. 29, pp. 34-45, 2018.

[23] Y.-D. Zhang, C. Pan, X. Chen, and F. Wang, "Abnormal breast identification by nine-layer convolutional neural network with parametric rectified linear unit and rank-based stochastic pooling," J. Comput. Sci, vol. 27, pp. 57-68, 2018.
[24] J. A. K. Suykens and J. Vandewalle, "Least squares support vector machine classifiers," Neural Process. Lett, vol. 9, no. 3, pp. 293-300, 1999.
[25] T. Cover and P. Hart, "Nearest neighbor pattern classification," IEEE Trans. Inf. Theory, vol. 13, no. 1, pp. 21-27, 1967.
[26] J. R. Quinlan, "Induction of decision trees," Mach. Learn, vol. 1, no. 1, pp. 81-106, 1986.
[27] X. Gu and P. P. Angelov, "Self-organising fuzzy logic classifier," Inform. Sciences, vol. 447, pp. 36-51, 2018.
[28] A. Krizhevsky, I. Sutskever, and G. E. Hinton, "ImageNet classification with deep convolutional neural networks," in Advances in Neural Information Processing Systems, vol. 25, 2012.
[29] C. Szegedy, "Going deeper with convolutions," 2015 IEEE Conference on Computer Vision and Pattern Recognition (CVPR), June 07-12, 2015.
[30] K. Simonyan and A. Zisserman, "Very deep convolutional networks for large-scale image recognition," 2014. [Online]. Available: arXiv:1409.1556.